Annales Societatis Geologorum Poloniae (2015), vol. 85: 187–203.

SUCCESSIVE STAGES OF CALCITIZATION AND SILICIFICATION OF CENOMANIAN SPICULE-BEARING TURBIDITES BASED ON MICROFACIES ANALYSIS, POLISH OUTER CARPATHIANS

Marta BĄK[1], Zbigniew GÓRNY[2,1], Krzysztof BĄK[3], Anna WOLSKA[1] & Beata STOŻEK[2]

[1] *Faculty of Geology, Geophysics and Environmental Protection, AGH University of Science and Technology, al. Mickiewicza 30, 30-059 Kraków, Poland; email: martabak@agh.edu.pl*
[2] *Institute of Geological Science, Jagiellonian University, Oleandry 2a, 30-063 Kraków, Poland*
[3] *Institute of Geography, Pedagogical University of Cracow, Podchorążych 2, 30-084 Kraków, Poland*

Bąk, M., Górny, Z., Bąk, K., Wolska, A. & Stożek, B., 2015. Successive stages of calcitization and silicification of Cenomanian spicule-bearing turbidites based on microfacies analysis, Polish Outer Carpathians. *Annales Societatis Geologorum Poloniae*, 85: 187–203.

Abstract: Mid-Cretaceous turbidites with large proportions of sponge spicules are widely distributed in the Silesian Nappe of the Outer Carpathians, giving rise to diversified types of sediments, from spiculites to spicule-bearing siliciclastics and calcarenites. Part of this succession, Middle–Late Cenomanian in age, was transformed into cherts. A microfacies study showed that these turbidite sediments underwent several stages of calcitization and silicification, which took place during Mid-Cretaceous times in different sedimentary environments, i.e., on a northern shelf bordering the Silesian Basin and on a deep sea floor. The first diagenetic changes were related to changes to the biotic components of the turbidite layers, dominated by siliceous sponge spicules. This process, which took place in the spiculitic carbonate mud on the shelves, was related to the calcitization of sponge spicules. Calcareous clasts and calcified skeletal elements also were corroded by bacteria. After transportation down the slope, the biogenic and siliciclastic particles were deposited below the carbonate compensation depth. Taphonomic processes on the basin floor and alternating phases of carbonate and silica cementations, recrystallization and dissolution occurred in these sediments and were related to the diversification in composition of successive turbidite layers. Silicification was related to the formation of quartz precipitates as fibrous chalcedony or microcrystalline quartz, which were derived from the earlier dissolution of amorphous silica, originating mostly from siliceous sponge spicules and radiolarian skeletons. However, a source of silica from hydrothermal vents was also possible. The initial silica precipitation could have taken place in a slightly acidic environment, where calcite was simultaneously dissolved. A number of silicification stages, visible as different forms of silica precipitate inside moulds after bioclasts, occur in the particular turbidite layers. They were related to changes in various elements of the pore-water profile after descending turbidity-current flows. A very low sedimentation rate during the Middle–Late Cenomanian in the Silesian Basin may have favoured the sequence of initial calcitization and silicification stages of the turbidite sediments.

Key words: calcitization, silicification, sponge spicules, spicule-bearing turbidites, cherts, Cenomanian, Outer Carpathians.

Manuscript received 20 August 2014, accepted 4 March 2015

INTRODUCTION

Spicule-bearing turbidites are very characteristic sediments, accumulated during the Cenomanian in the Outer Carpathian basins of the Tethyan domain, spreading out along the southern edge of the European Platform (Sujkowski, 1933; Książkiewicz, 1951, 1956; Unrug, 1959; Alexandrowicz, 1973). Sponge spicules are the main components of medium- to thick-bedded turbidites in gaize, spiculite and chert layers in medium- to thick-bedded turbidites. The Middle–Upper Cenomanian sediments in the Silesian and Subsilesian nappes of the Outer Carpathians, named the Mikuszowice Cherts, are an example of such facies extending along the Outer Carpathians are over a distance of more than 300 km (e.g., Burtanówna, 1933; Książkiewicz, 1951; Burtan and Skoczylas-Ciszewska, 1956; Koszarski and Nowak,1960; Koszarski and Ślączka, 1973). The siliceous sponge spicules with radiolarians, foraminifers, and siliciclastic and calcareous material create a series of fine-grained turbidites in this unit, intercalated with hemipelagic, non-calcareous clays (Bąk M. *et al.*, 2011).

This paper focuses on well developed and well exposed spicule-rich turbidites in the central part of the Silesian Ba-

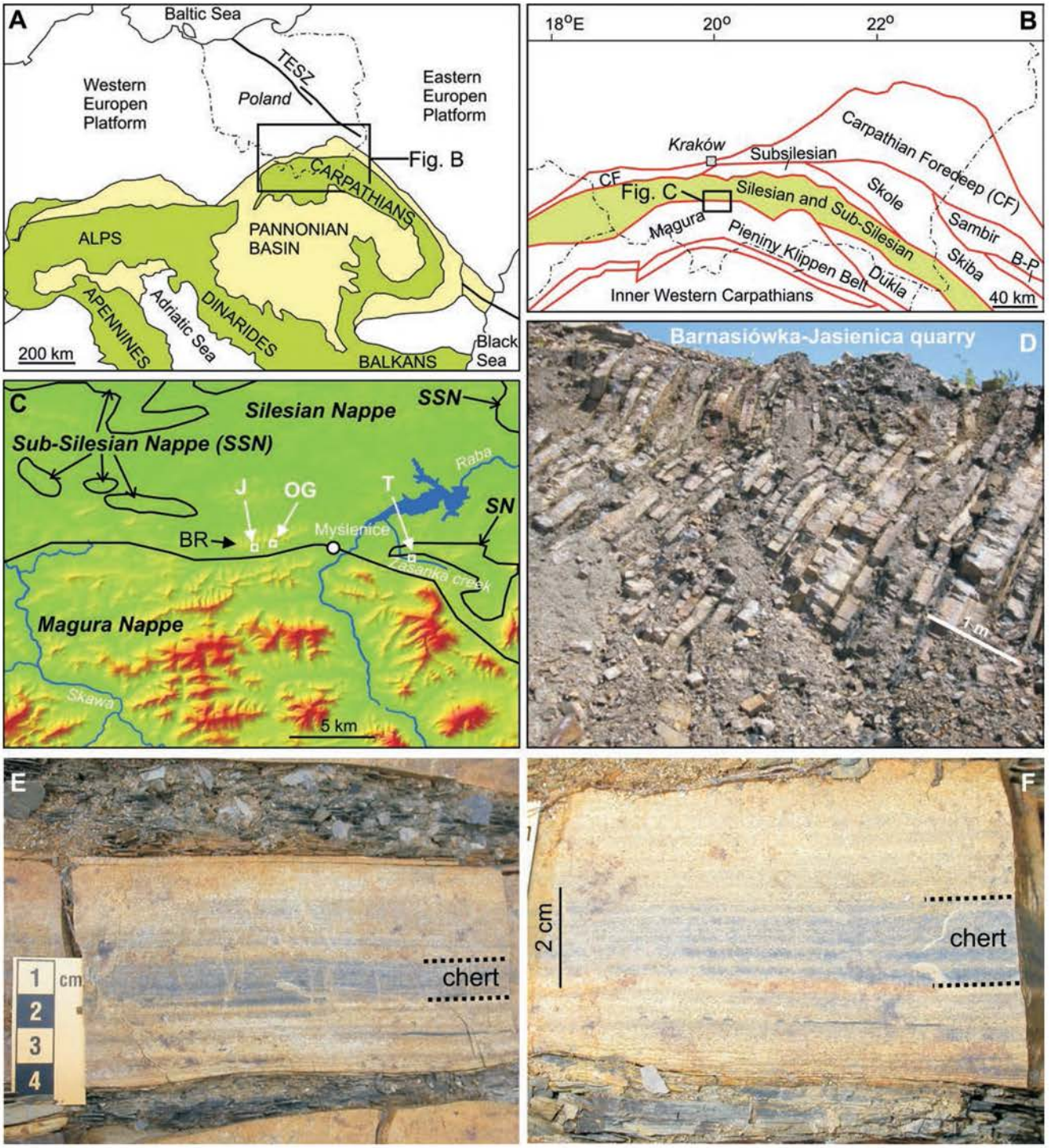

Fig. 1. Location of the study area. **A.** The Carpathians against the background of a simplified geological map of the Alpine orogeny and their foreland. **B.** Tectonic sketch map of the Western Carpathians with location of the Silesian and Sub-Silesian nappes. **C.** Location of the sections studied in the Silesian Nappe of the Outer Carpathians against the background of a contour map (Bryndal, 2014); boundaries of structural units after Oszczypko (2004): J – Barnasiówka-Jasienica Quarry, OG – Ostra Góra Quarry, T – Trzemeśnia; BR – Barnasiówka Ridge. **D.** Example of succession of spicule-bearing turbidites (thick-bedded sandstone layer) in the upper part of the Mikuszowice Cherts (Upper Cenomanian) exposed in the Barnasiówka-Jasienica Quarry. **E, F.** Example of a single spicule-bearing sandstone with a chert layer.

sin of the Outer Carpathians (Fig. 1). Previous field and microscope observations (Bąk M. *et al.*, 2005, 2011) indicated that these sediments had undergone several stages of diagenetic processes with carbonate and siliceous cementation, leading to the formation of numerous chert layers. The cherts occur as thin layers in the medium- to thick-bedded turbidite sandstones.

Silicification events producing microcrystalline quartz through the transformation of biogenic amorphous opal-A was suggested by many authors with regard to various sedi-

mentary rocks. Review articles related to this problem include those by: Williams and Crerar (1985), Williams *et al.* (1985), Hesse (1989), and Knauth (1994). The chemical and mineralogical changes occurring in this transformation process were presented on the basis of experimental investigations (e.g., Mizutani, 1970) and commonly in relation to studies of oceanic sediments in the Deep-Sea Drilling Project (e.g., Calvert, 1971; Von Rad and Rösch, 1972, 1974; Hurd, 1973; Calvert, 1974; Wise and de Weaver, 1974; Keene, 1975; Riech and von Rad, 1979; Hurd *et al.*, 1981; Baltuck, 1986; Cady *et al.*, 1996), turbidite sediments (Elorza and Bustillo, 1989) and the chalk facies of epicontinental seas (e.g., Clayton, 1986; Zijlstra, 1987; Madsen and Stemmerik, 2010).

The aim of this study is to elucidate the processes and environment that led to the diagenetic transformations of biogenic particles, which are components of the turbidites, and to determine the diagenetic history of the spicule-bearing sediments after their deposition in a deep-sea environment.

This study is based on microfacies analysis, in conjunction with SEM observations on the biogenic particles of silty/sandy turbidites and also the sequences of generation of cement and dissolution of various particles, which took place before their deposition and after their burial.

GEOLOGICAL BACKGROUND

The study area is located in the central part of the Silesian Nappe in the Outer Carpathians (Fig. 1A–C), in the Lanckorona-Żegocina tectonic zone (Książkiewicz, 1951; Koszarski and Ślączka, 1973). During the Cretaceous, the sediments of the Silesian Nappe accumulated in the northern part of the Carpathian basins, known as the Silesian Basin, restricted to the south by the Silesian Ridge (cordillera) and to the north by the southern shelves of the West European Platform or the Sub-Silesian submerged ridge (Książkiewicz, 1962).

Mid-Cretaceous sedimentation of the spicule-bearing turbidites in this area began with the accumulation of the Albian–Lower Cenomanian Middle Lgota Beds (Książkiewicz, 1951; Unrug, 1959) and came to an end during deposition of the Turonian Variegated Shale, with an interruption during the uppermost Cenomanian–lowermost Turonian, related to Oceanic Anoxic Event 2 (OAE2; Bąk, 2007a; Okoński *et al.*, 2014). The detrital material was supplied by turbidite currents from the shelves and slopes of the West European Platform, as documented by the orientation of the flute casts of sandstone layers (Książkiewicz, 1962; Unrug, 1977). Numerous biogenic particles with large amounts of sponge spicules occurring in these turbidites originated from the growth and destruction of sponge communities, built of the rigid skeletons of sponges mostly of lithistids group, and formed on the same shelves. The detrital grains and biogenic particles of the turbidites correspond mostly to the $T_{b\text{-}d}$ divisions of the classic Bouma sequence (Bąk M. *et al.*, 2011). They are commonly graded, with sand/silt passing upwards into mud. The biggest particles are loose sponge spicules, with an average maximum dimension ranging from 100 to 200 μm.

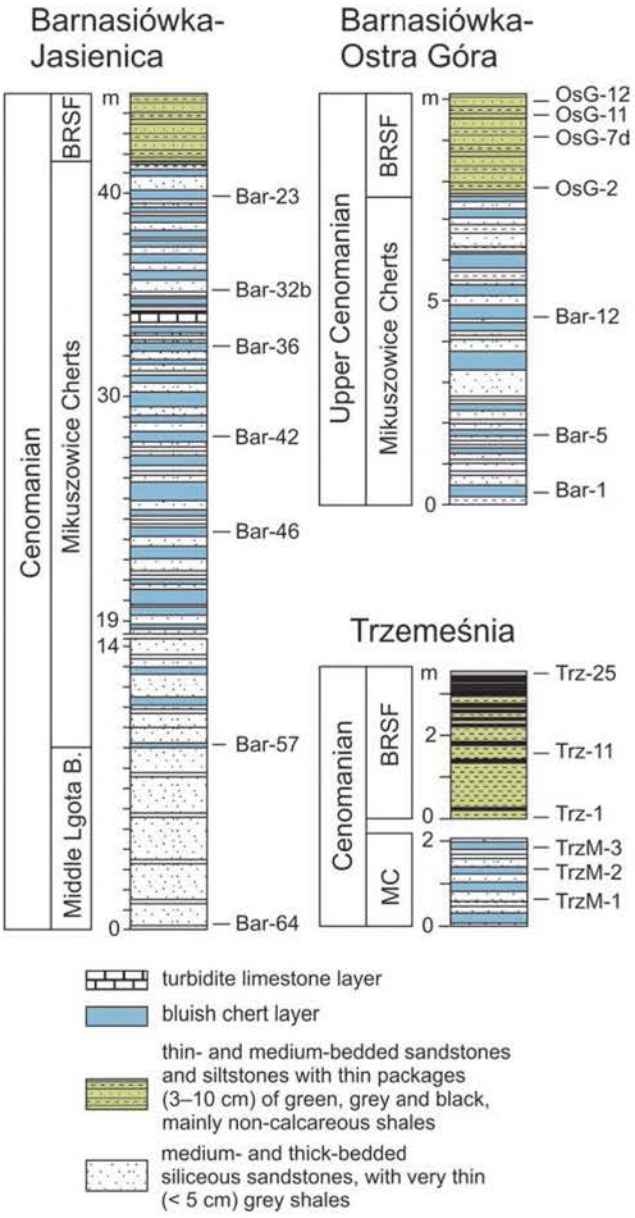

Fig. 2. Stratigraphic logs of the Mikuszowice Cherts (MC) and the encompassing units at the Barnasiówka-Jasienica, Barnasiówka-Ostra Góra and Trzemeśnia sections, with locations of the samples studied. Numbered samples are related to photographs in Figures 3–6. BRSF–Barnasiówka Radiolarian Shale Formation.

The spicule-bearing turbidites studied belong to three lithostratigraphic units: the Middle Lgota Beds, the Mikuszowice Cherts (the so-called Upper Lgota Beds) and the Barnasiówka Radiolarian Shale Formation (Fig. 2). Generally, all of them are dominated by turbidite sandstones, mudstones and claystones, with intercalations of non-calcareous, green to black shales. The Middle Lgota Beds (Aptian–Lower Cenomanian; Geroch *et al.*, 1967; Bąk M. *et al.*, 2005) consist mainly of thin-bedded turbidites with very thin, hemipelagic, partly siliceous clays. The most characteristic feature of the overlying Mikuszowice Cherts (Middle–Upper Cenomanian; Bąk M. *et al.*, 2005) is the occurrence of bluish chert layers in the middle and upper parts of medium- and thick-bedded, fine-grained sandstones (Fig. 1E, F). In turn, the Bar-

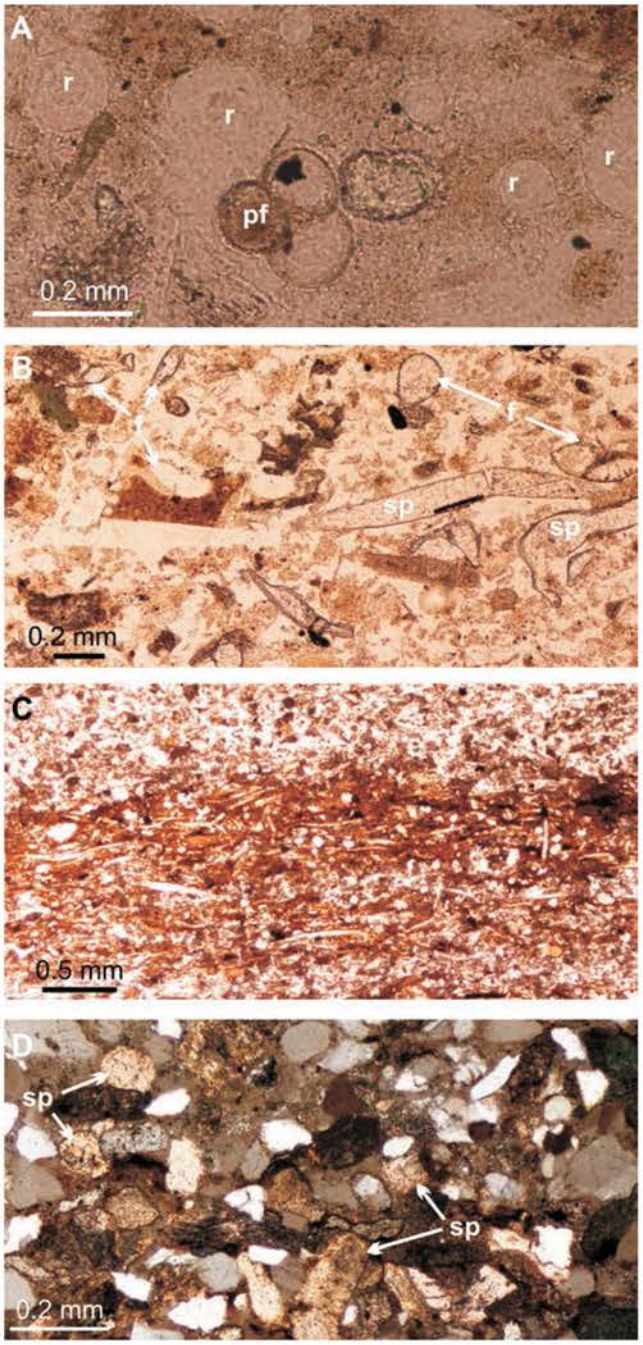

Fig. 3. The most characteristic microfacies of spicule-bearing turbidites occurring in the Middle Lgota Beds and Mikuszowice Cherts (A–C: plane light; D: crossed polars). **A.** Biomicrite with radiolarians (r) and planktonic foraminifer (pf); sample Bar-5. **B.** Biomicrite with benthic foraminifers (f) and sponge spicules (sp); sample Bar-5. **C.** Spiculitic sublitharenite; sample Bar-57. **D.** Sublitharenite with calcified spicules (sp); sample Bar-64.

nasiówka Radiolarian Shale Formation (Upper Cenomanian–lowermost Turonian; Bąk K. *et al.*, 2001) consists of thin-bedded silty and muddy turbidites, with thicker intercalations of hemipelagic, green to black claystones. The succession of turbidites directly precedes the uppermost Cenomanian black, organic-rich shales, representing the sediments of OAE2 (Bąk K., 2006, 2007a–c; Bąk M., 2011).

MATERIAL AND METHODS

Three sections including the spicule-bearing turbidites, which belong to the Cenomanian sediments of the lithostratigraphic units mentioned above, were sampled with microfacies studies in mind. Two of them, the Barnasiówka-Jasienica (Fig. 1D) and the Barnasiówka-Ostra Góra are exposed in quarries at the Barnasiówka Ridge (2 km away), near Bysina and Jasienica villages, a few kilometres west of Myślenice town (Fig. 1C). A third one, the Trzemeśnia section, is exposed near the mouth of a right tributary of Zasanka Creek, in Trzemeśnia village (Fig. 1C). The detailed location of the sections studied and their relationship to the regional geology was presented by Bąk K. *et al.* (2001). The location of the samples used in this study (Fig. 2) is the same as that presented in papers by Bąk M. *et al.* (2005) for the Barnasiówka-Jasienica and Barnasiówka-Ostra Góra sections, and by Bąk K. (2007a) for the Trzemeśnia section.

The microfacies and microfossils were determined and analysed in forty-six thin sections, made from eighteen samples of the sandstones. The replacement textures as well as silica and carbonate cementations observable in thin sections were described. These textures were interpreted with respect to the composition of biogenic (carbonate and siliceous) sediment particles.

Selected mineral constituents of the sponge spicules were studied by electron microprobe point analyses, using a Hitachi S-4700 SEM with a link Noran Vantage EDS (the data were corrected using the ZAF/PB programme). The sponge spicules used in this analysis were extracted from the turbidite sandstone layers. They came from pieces weighing about 200 g, which were treated with 3–5% hydrofluoric acid. The residues (1–3 g) were dried, weighed and washed through sieves with mesh diameters of 63–500 μm.

Thin sections of the rock used in microfacies analyses and cells with sponge spicules are housed in the Faculty of Geology, Geophysics and Environmental Protection, at the AGH University of Science and Technology, Kraków, Poland.

RESULTS

General sedimentary features of turbidites

A single turbidite layer in the successions studied represents a sequence of various lithotypes, resulting from current sorting of particles with various shapes, weights and different specific gravities. One depositional turbidite event may contain successively (Fig. 3): (1) detrital grains such as quartz and/or lithic grains, usually forming sublitharenite, which passes upwards into (2) sublitharenite with increasing content of biogenic particles such as sponge spicules and calcareous benthic foraminifers, (3) spiculitic sublitharenite, (4) spiculite, which usually passes into (5) lithotypes containing more micrite/sparite with increasing amounts of planktonic foraminifers and radiolarians. These sequences finally pass into a hemipelagite layer, corresponding to deep-water pelagic sedimentation and containing agglutinated benthic foraminifers and radiolarians, but devoid of calcareous micro-/nannofossils. The boundaries between the lithotypes mentioned above usually facilitated the later silicification process during the diagenetic remobilisation of silica.

Distribution of microfacies in the lithostratigraphical units studied

The Middle division of the Lgota Beds is composed of centimetres-thick, diagenetically altered beds (up to 25 cm thick) of fine- to medium-grained, dark grey and black sublitharenites, siliceous shales and biomicrites, partly silicified, in packages up to 20 cm thick. The coarser material in the turbidite layers generally represents sublitharenites, in places containing calcareous benthic foraminifers and sponge spicules. The finest calcarenitic material corresponds to biointramicrites and mudstones.

The Mikuszowice Cherts are the main body of the spicule-bearing turbidites. They are composed of centimetre-thick layers, which are fine-grained siliciclastics as sublitharenites, mudstones and siltstones with biogenic admixture, and also calcarenites to calcisiltites, usually silicified. In some places, the siliciclastics pass into carbonate sediments with variable detrital admixtures. The microfacies composition shows the following types: (1) fine- to medium-grained sublitharenite with calcitic matrix/cement, in places with a biogenic admixture, (2) sublitharenite with sponge spicules containing 5–10% of sponge spicules, (3) spiculitic sublitharenite, (4) spiculite containing up to 90% of sponge spicules, with rare foraminifers and radiolarians and very rare detrital grains which are quartz and glauconite, and (5) biomicrite/sparite with radiolarians, planktonic and benthic calcareous foraminifers, and rare sponge spicules. Pure sublitharenites, sublitharenites with a biogenic admixture, and spiculitic sublitharenite are the most common microfacies in the upper part of the Mikuszowice Cherts.

The lower part of the Barnasiówka Radiolarian Shale Formation is the unit, which marks the final occurrence of spicule-bearing turbidites within the Cenomanian succession. These sediments are composed of centimetres-thick layers (up to 12 cm thick), in which fine-grained siliciclastics as sublitharenite, mudstones and siltstones occur, with a biogenic admixture, and calcarenites to calcisiltites, usually silicified.

Petrographic features of biogenic and inorganic components in turbidites

The turbidites include mainly sponge spicules within the biotic components. Less common are radiolarians, planktonic and calcareous benthic foraminifers, inoceramid prisms, and echinoderm ossicles. Chert layers in the turbidites display a similar composition of biogenic particles, although the siliceous microfossils are much better preserved.

Sponge spicules

Spicules of sponges recognised in the material studied belong to two taxonomic groups of siliceous sponges in the class level as Demospongea Sollas 1875 and Hexactinellida Schmidt 1870 (Bąk M. *et al.*, in press). Most spicules belong to the lithistid demosponges, which are classified as the polyphyletic (informal) group of class Demospongea, characterized by rigid skeletons composed of desmas spicules (e.g., Pisera and Lévi, 2002). Spicules predominate among the biogenic components (Figs 3, 4), ranging from 10 to 60% of their total volume. They were originally made up of hydrated, amorphous, noncrystalline silica (opal-A); however this did not occur in the material studied. The characteristic feature of the spicule was an open axial canal, circular in outline (Fig. 4A, N). Spicules in the sediments studied represent two main types of preservation. They are (1) replaced by blocky calcite (Figs 4I, J, O–R, 5) and (2) replaced by various phases of silica (Fig. 4L, M1, M2).

(1) Replacement by blocky calcite represents the predominant type of preservation of spicules. Various cross-sections and SEM observations including EDS measurements show that calcite very consistently replaced the whole spicule (Fig. 5). The axial canal of the spicule is usually obscured and filled in by the same type of calcite cement as the outer part of the spicule (Fig. 5E). However, some of the calcified spicules display a well preserved open canal (Fig. 4N).

(2) Spicules replaced by more stable silica phases are rare in the Lower–Middle Cenomanian part of the succession studied and their numbers increase in the Upper Cenomanian turbidites, where they predominate among the biogenic clasts. They are composed of microcrystalline quartz (Fig. 4D–H, K–M2) or fibrous quartz (Fig. 4E, M2). An axial canal has not been preserved in most of the spicules.

Radiolarians

Radiolarians are common in the turbidite layers, but poorly to moderately preserved (Fig. 6A–C). Only 15% of the skeletons are identifiable. The number of individuals varies, depending on the type and derivation of the host-sediment. They are numerous in the sand fraction within the turbidites studied, even exceeding 10 000 individuals per 100 g of the rock sample. Their skeletons are mostly recrystallized or present as voids, cemented by calcite (Fig. 6B1, C).

Foraminifers

The content of calcareous (benthic and planktonic) foraminiferal tests ranges from 1 up to 10% of the entire microfacies content. Benthic foraminifers are usually present as voids, reduced in volume by infillings of calcite cement (Fig. 6D–F). Their primary walls were replaced by fringe sparite (Fig. 6D–F2). Some of them are empty, but usually they are filled with calcitic or siliceous cement (Fig. 6D–K). The tests of planktonic foraminifers were usually replaced by fringe sparite (Fig. 6D) or a micritic envelope (Fig. 6I–K).

Microborings

Post-mortem microborings of carbonate bioclasts and some of carbonate intraclasts by bacteria are also characteristic of the material studied. Many tests of planktonic and benthic foraminifers, and calcified demosponge spicules have a micritic halo (Fig. 6I–K) around their outer margins, which is a combination of the microboring process and the later infilling of the borings with cryptocrystalline calcite.

Pyrite framboids

Spherical pyrite framboids are attached directly to the inner surfaces of foraminiferal tests, both planktonic and benthic (Fig. 6E–F2, I–K). They could be in contact with calcite cement, reducing the porosity of the test. Addition-

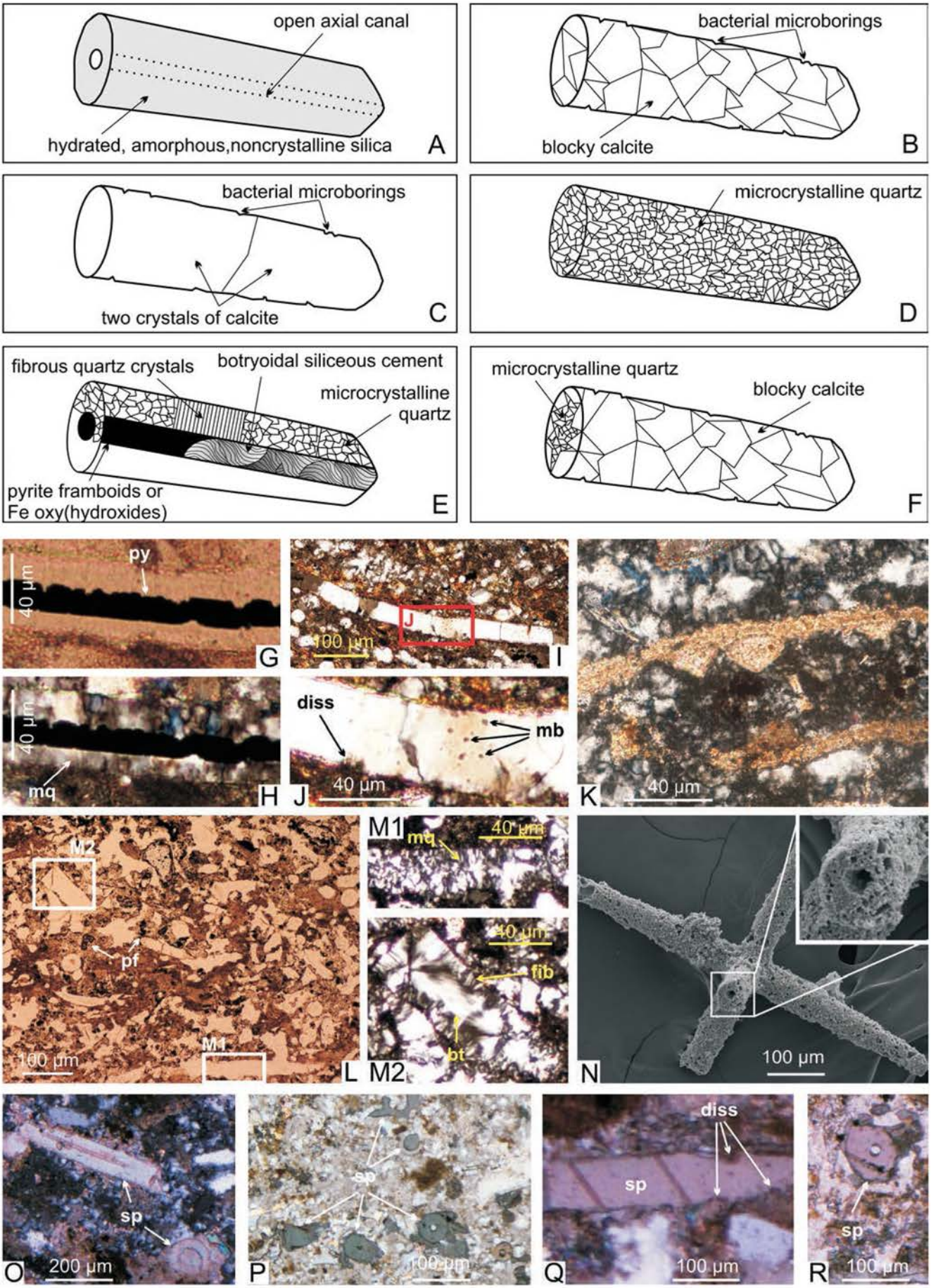
open axial canal
hydrated, amorphous,noncrystalline silica
A
bacterial microborings
blocky calcite
B
bacterial microborings
two crystals of calcite
C
microcrystalline quartz
D
fibrous quartz crystals
botryoidal siliceous cement
microcrystalline quartz
pyrite framboids or Fe oxy(hydroxides)
E
microcrystalline quartz
blocky calcite
F
py
40 µm
G
100 µm
J
I
40 µm
mq
H
diss
mb
40 µm
J
40 µm
K
M2
pf
100 µm
M1
L
M1
mq
40 µm
40 µm
fib
bt
M2
100 µm
N
sp
200 µm
O
sp
100 µm
P
diss
sp
100 µm
Q
sp
100 µm
R

ally, the framboids are located between calcite crystals, which partly replaced the foraminiferal test wall (Fig. 6K). Moreover, the pyrite framboids may infill the central part of a sponge spicule left after the primary stage of silica cementation (Fig. 4E, G, H).

Matrix

The content and composition of the matrix change along individual turbidite layers and differ between particular turbidites within the succession studied. The matrix consists mostly of detritic clay minerals, micrite, rhombic dolomite crystals and organic matter in the turbidites of the Middle Lgota Beds (Fig. 6B–D), with an increasing amount of carbonate and Fe-oxides in the underlying parts of the succession studied. The carbonate matrix (primary micrite) is usually visible as recrystallized in the form of sparite and blocky calcite, or it was partly replaced by chalcedony and microcrystalline quartz (Fig. 6D).

Calcareous and siliceous cements

Carbonate cement is represented by rhombic calcite and dolomite crystals and as micrite, showing different degrees of recrystallization (Fig. 7C, D). Rhombic calcite-like crystals and rare dolomite crystals occur in a contact with microquartz and chalcedony, which fill in different types of porosity in the sediment. Calcite crystals formed syntaxial overgrowths on the calcified spicules of sponges (Fig. 5B–F).

Silica cement usually filled in the earlier voids left after the dissolution of calcareous bioclasts and the calcified spicules of siliceous sponges. Some of these particles were previously overgrown by syntaxial calcite (Figs 7H, 8A–F), then fibrous chalcedony and microcrystalline quartz precipitated in the voids (Fig. 7C, D, I, J). Chalcedony and microquartz also replaced calcite rhombohedra and the primary micritic matrix (Fig. 7G–K).

Structures left after mechanical compaction

Some of the internal structures in the turbidite layers remained after previous mechanical compaction. Silicified rocks usually display load-cast structures, indicating silicification after early mechanical compaction. Other lines of evidence are microfracturing of some sponge spicules (Fig. 4I), calcite crystals (Fig. 8), sutured contacts between quartz and glauconite grains or individual carbonate grains (Fig. 9A, B), plastic deformation of lithic fragments (Fig. 9A) and deformation of mica flakes (Fig. 7B).

Structures left after chemical compaction

The main structures produced by chemical compaction are seams and stylolites caused by pressure solution. Stylolites are present in the carbonate-rich beds that contained a predominantly carbonate matrix. The stylolites separate particles with an insoluble residue (clay minerals, iron oxides, and organic matter; Fig. 7E, F). Small stylolites occur usually in the biointramicrites, where quartz, silt and small opaque grains have accumulated as a residue after pressure dissolution.

Occurrence and petrography of cherts

The outstanding feature of these deposits is the occurrence of light grey and bluish cherts in the Mikuszowice Cherts (Fig. 1E, F), but they also are present in the Middle Lgota Beds. The cherts form layers from millimetres up to several centimetres in scale, and account for up to 50% of the bed. The cherts are parallel-laminated, similar to the host sediment (Fig. 1E, F). Thin sections show that the morphology of the chert layers is controlled by the primary sediment composition, sedimentary structures and porosity. The cherts may have sharp contacts with the underlying sediments and pass through the overlying one. Initially, silica replaced very consistently carbonates in form of micrite and/or sparite. Most of the silica is in the form of microcrystalline minerals (microquartz, megaquartz, and chalcedony; e.g., Hesse, 1989; Flörke *et al.*, 1991; Heaney, 1993).

In the sediments studied, microquartz is characterized by mosaics of equal-sized crystals, up to 20 μm across, with undulatory extinction. Microquartz usually replaced carbonate sediment, and bioclasts, and is the first cement generation to fill primary intraparticle porosity. Megaquartz is

Fig. 4. Various preservation stages of sponge spicules observable in thin sections of spicule-bearing turbidites, Outer Carpathians. **A.** Generalized morphology of a siliceous sponge spicule. **B–F.** Drawings showing the types of recrystallization and replacement of sponge spicules present in the material studied. **G, H.** The same photomicrograph under plane light (G) and crossed polars (H), showing successive stage of silica crystallization in void after sponge spicule. The process started with partial overgrowing by microcrystalline silica (mq) from outside toward the inner part of the void. The pyrite crystals (py) grew in the emptiness left after silicification; sample TrzM-3. **I.** Spicule of siliceous sponge replaced by blocky calcite; sample TrzM-1. **J.** Close-up view of Figure I showing bacterial-size microborings (mb) present along the spicule outline. Outer spicule surface visible on cross-section possesses signs of dissolution (diss). Rounded shape of the voids indicates that this process took place when spicule was originally siliceous. **K.** Cross-section of benthic foraminifera test with original wall replaced and partly covered by sparite. The first stage of infilling involved calcite-like crystals, which grew attached to the inner wall. Quartz microcrystals grew during secondary cementation stage; Sample OsG-2. **L.** Another view of spiculite microfacies showing that most of spicule moulds are strongly corroded. Planktonic foraminifers (pf); sample Bar-12. **M1.** Close-up view of Figure L under crossed polars, showing that moulds are completely filled by microcrystalline quartz (mq). **M2.** Another close-up view of Figure L showing cross-section through mould after spicule, which was formed during two stages of silica precipitation. First stage (1) left rim of microquartz grain along the outermost wall of a previous void. During second stage (2), an empty space left inside void and imitating the spicule axial canal, was infilled with chalcedony; sample Bar-12. **N.** Spicule of Hexactinellid sponge replaced by calcite crystals. The remnants of axial canal are visible inside the spicule; sample Bar-12. **O–R.** Photomicrographs of sublitharenite with spicules of sponges, showing different cross-sections of calcified, previously siliceous spicules, replaced by blocky calcite (sp); sample Bar-37. **Q.** Calcified spicules of previously siliceous sponge. Outer spicule surface possess semicircular, concave hollows, left after dissolution (diss).

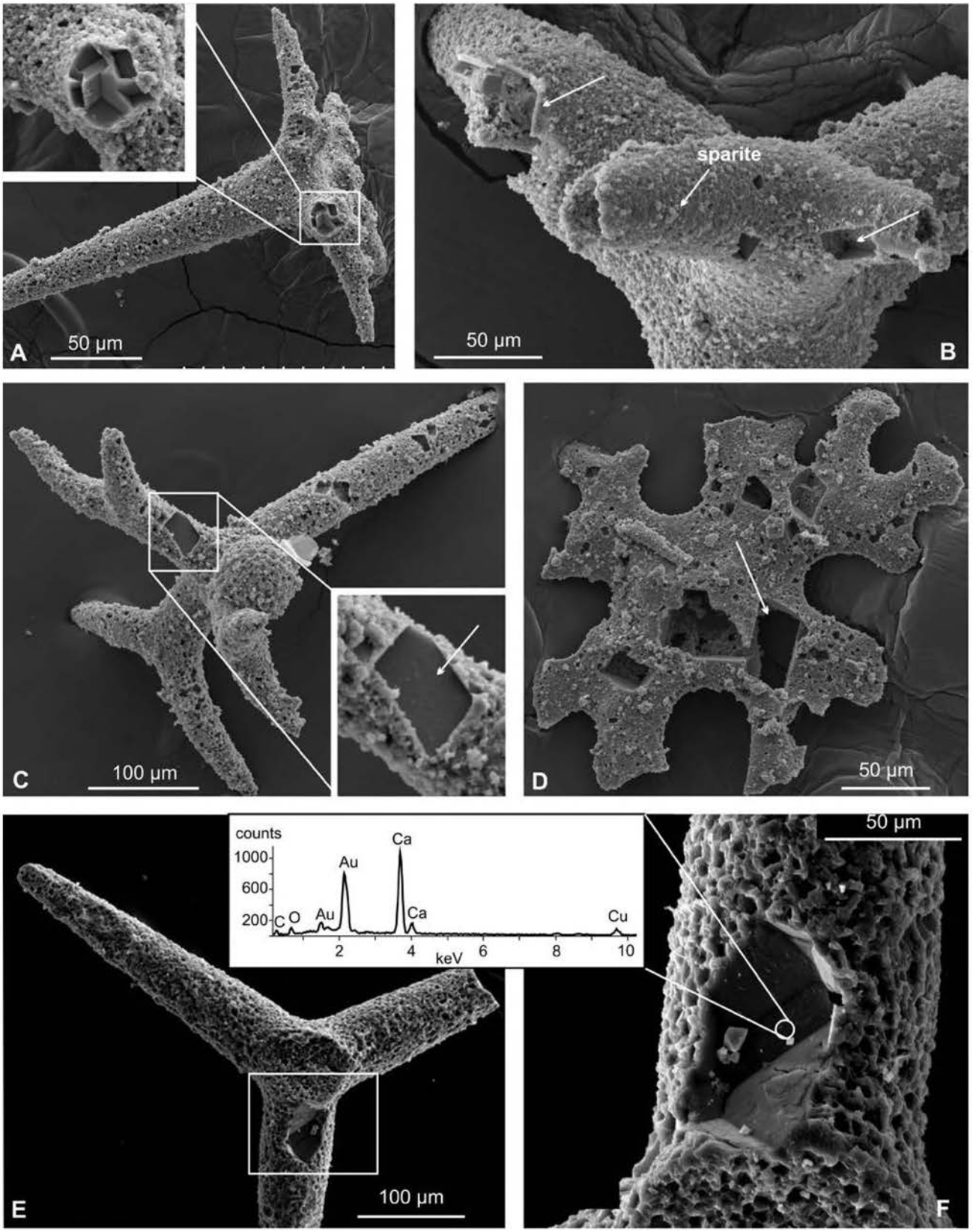

Fig. 5. Spicules of sponges, etched by weak solution of hydrofluoric acid from chertified spiculites. All spicules are preserved as moulds after the original silica, now filled in by calcite crystals. **A–C.** Phyllotriaene spicules. **A.** Broken part of the spicule indicates that inner part consists of densely packed calcite crystals. **B.** Close-up view showing outermost part of the mould after spicule, which consists of small calcite crystals (sparite), less than 10 µm across. Cavities in rhombohedral shape (arrows) left after syntaxial cement. **C.** Photomicrographs showing that spicule mould surface possesses cavities in rhombohedral shape (arrow) left after syntaxial cement. **D.** Flat dermal spicule preserved as mould with several pores with rhombic shape (arrows) after syntaxial calcite cement overgrowth. **E, F.** General view of spicule mould (**E**) and close-up of calcite crystals with point of EDS analysis. Specimens covered by Au coatings for analysis. All samples – Bar-36.

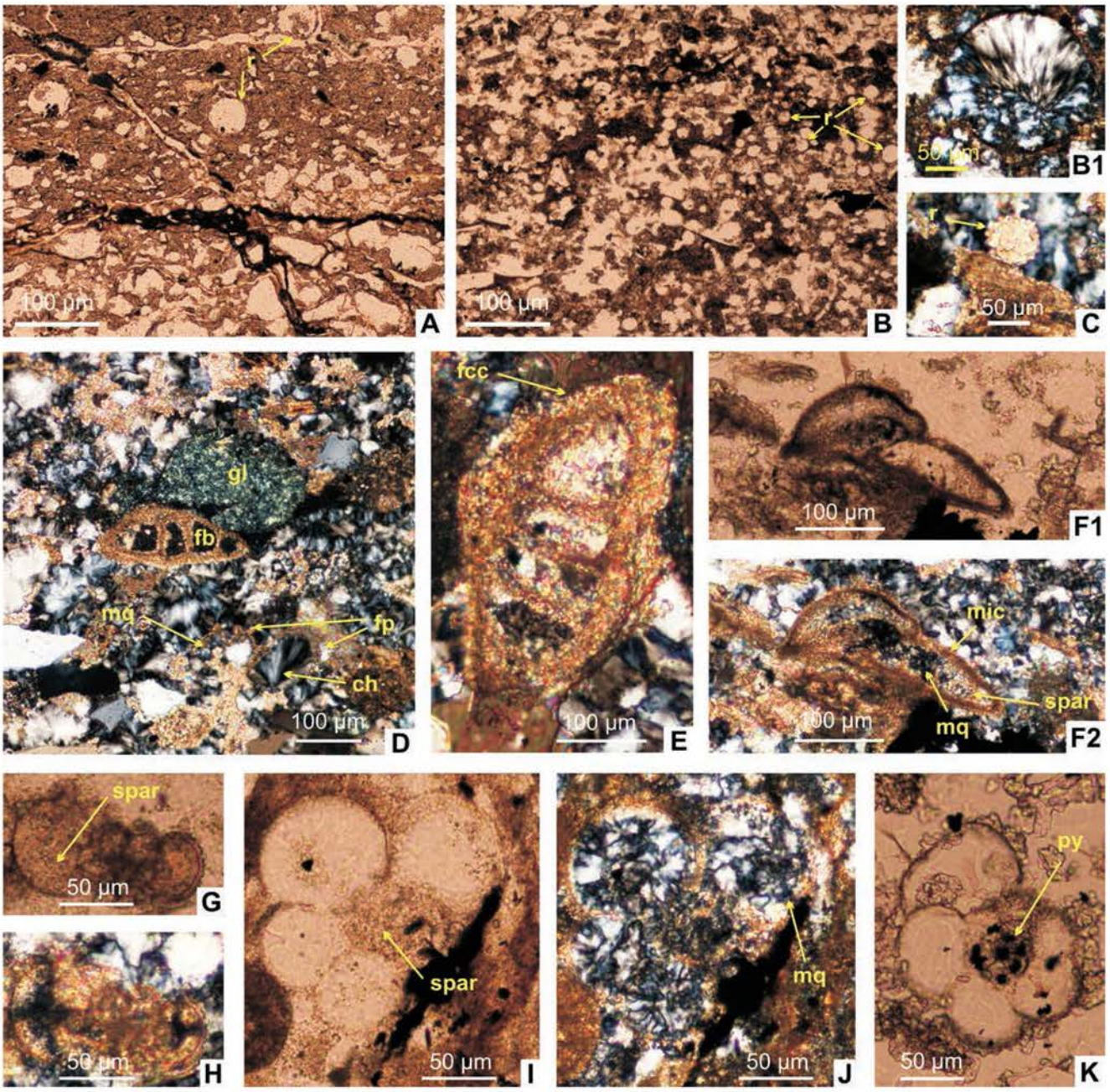

Fig. 6. Bioclasts in spicule-bearing turbidites. **A, B.** Spiculitic sublitharenite with common radiolarian skeletons, which are recrystallized and usually filled in with microcrystalline silica; A – sample OsG-7d; B – sample OsG-12. **B1.** Close-up view of sample OsG-12 with crossed polars, showing fibrous microcrystalline silica filling in radiolarian test. **C.** Radiolarian species from genus *Praeco- nocaryomma* replaced and filled in with blocky calcite; sample OsG-7d. **D.** Original biomicrite with benthic (fb) and planktonic (fp) foraminifers, and rare glauconite (gl) grains after stages of calcitization and silicification. Foraminiferal calcareous tests are recrystallized into sparite. Micritic matrix was secondarily recrystallized into sparite or replaced by chalcedony and microcrystalline quartz. Planktonic foraminiferal tests are filled in with chalcedonic cement (ch) or microquartz (mq); sample OsG-10. **E.** Calcareous benthic foraminifer from genus *Gyroidinoides* with test recrystallized by spar and partly covered by fringe calcite cement (fcc – whitish crystals in external part of wall); sample OsG-2. **F1, F2.** Calcareous benthic foraminifer from genus *Gavelinella/Lingulogavelinella* with chamber walls micritized (mic) and filled in partly with sparite (spar) and microcrystalline quartz (mq); sample OsG-12. **G–K.** Different preservation states of planktonic foraminifers from genus *Hedbergella*. An original test recrystallized in sparite (G, H) and filled with microquartz (mq) (J). Inner chambers contain pyrite framboids (py), attached to chamber wall or calcite, which crystallized inside the chambers (K); H–K – sample OsG-11.

characterized by mosaics of crystals up to 300 µm in diameter. It always occurs as a late cement after generations of microquartz and chalcedony and as the primary and secondary fillings of voids after calcified spicules and foraminiferal chambers. It is also present as a secondary generation of pseudomorphs after rhombohedral-calcite-like crystals. The fibrous variety of quartz is less common. Chalcedony is present locally as a cement phase, mostly botryoidal.

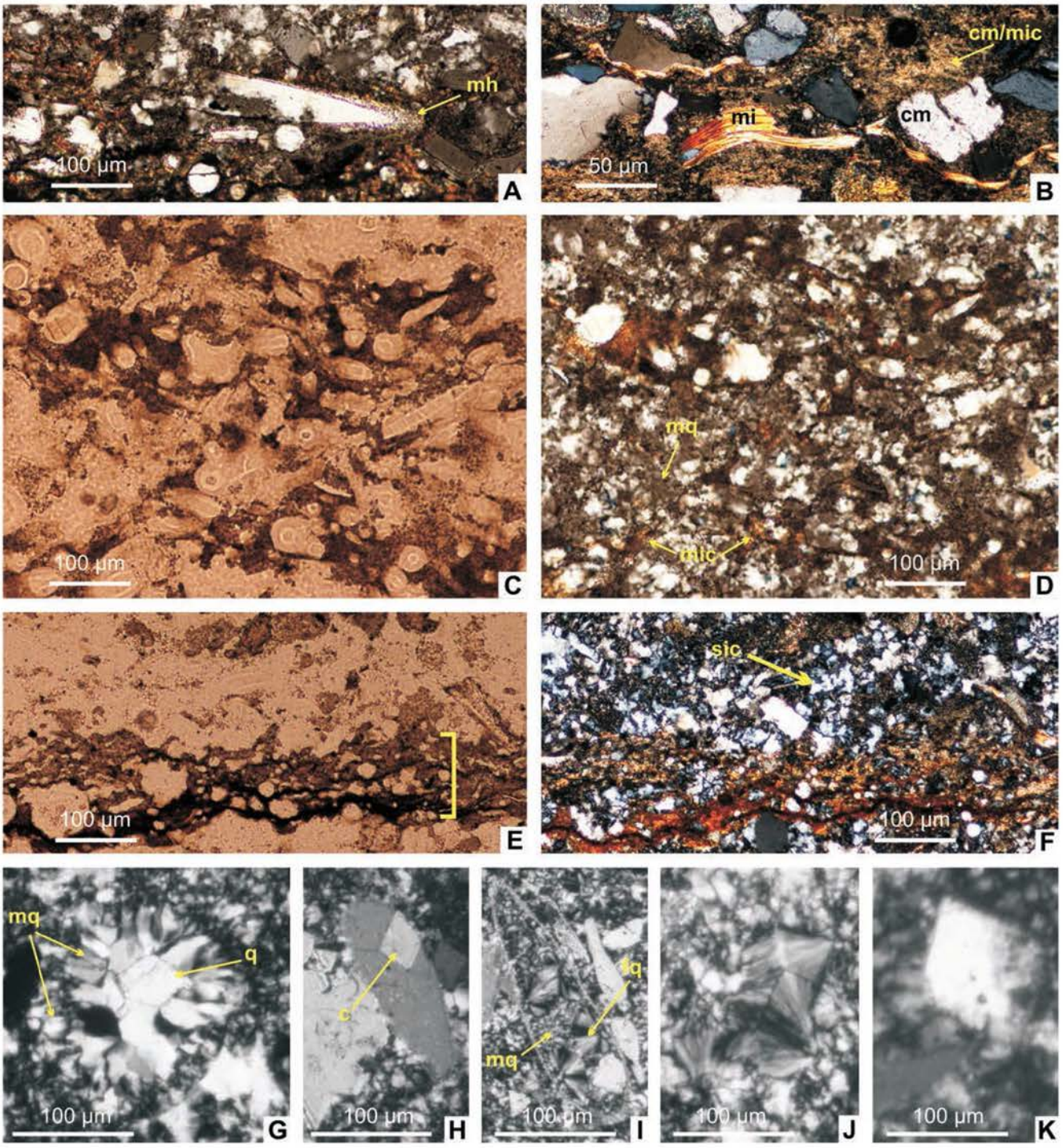

Fig. 7. **A.** Spicule of siliceous sponge in sublitharenite, which was replaced by blocky calcite. Micritic halo (mh) around outer margins of spicule, as a result of microboring, filled with cryptocrystalline calcite; sample Bar-30. **B.** Sublitharenite with matrix consisting of clay minerals (cm), and micrite (mic). Plastic deformation of micas flakes (mi) formed after mechanical compaction; sample Trz-11. **C, D.** Spiculitic sublitharenite with moulds after originally siliceous sponge spicules, surrounded by two generations of cements (as microquartz) and micrite (mic); sample Bar-32b. **E, F.** Two photomicrographs of microstylolite under plane and crossed polars. Microstylolite was formed in layer with prevailing carbonate matrix (yellow buckle). It separates particles which consist of insoluble residue as clay minerals, iron oxides, and organic matter; sample Bar-23. **G.** Cross-section of moulds after radiolarian test contains microquartz (mq) and calcite-like crystal inside fill of one quartz crystal (q). **H.** Void after previously siliceous spicule of sponge filled in with calcite cement. One small calcite crystal is attached to inner wall (c). **I.** Foraminiferal test filled with microquartz (mq) and fibrous quartz, which were precipitated in rhombic space (fq).

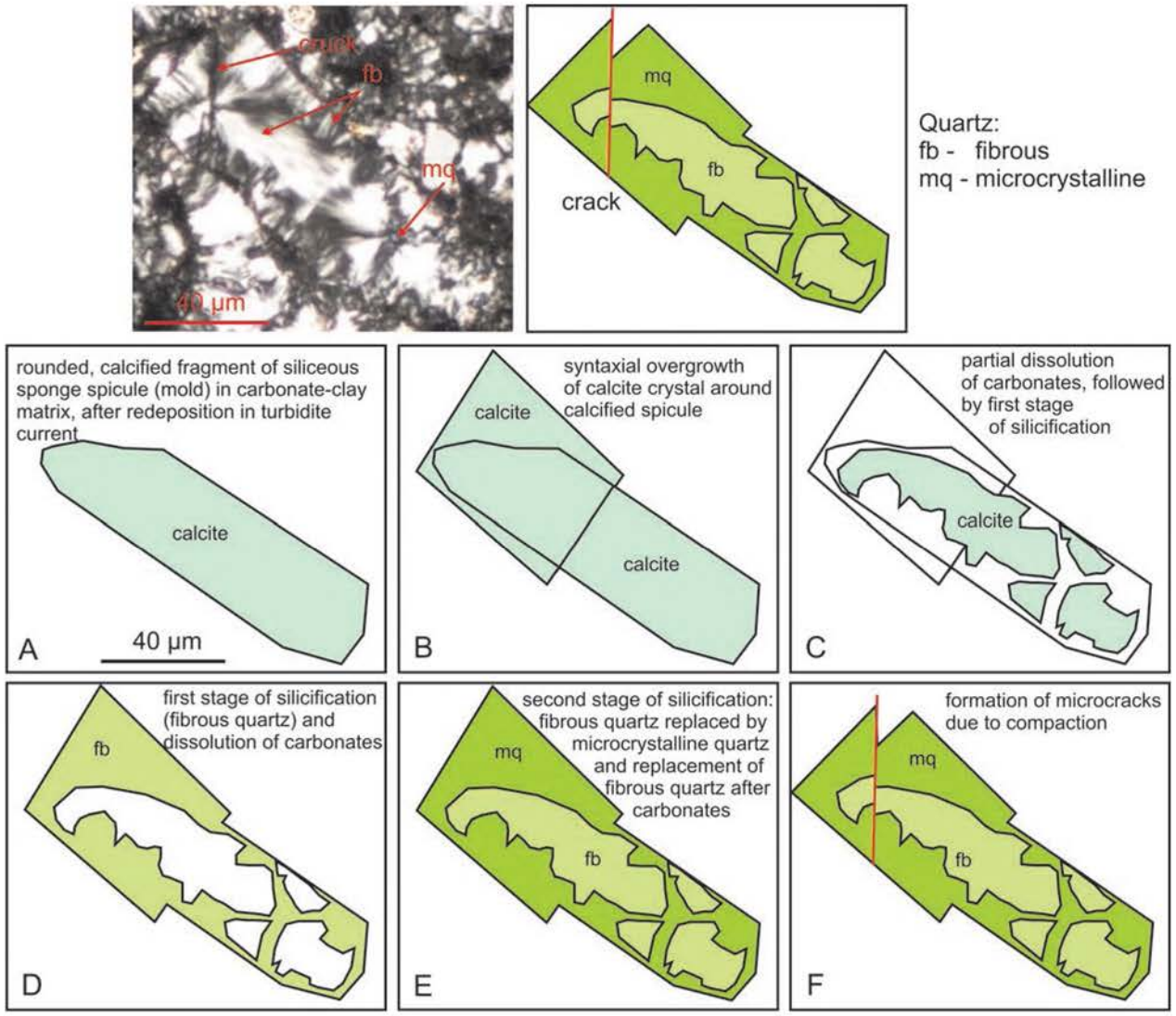

Fig. 8. Time-spatial model of early diagenetic processes which took place in neritic and slope environments of the Silesian Basin

DISCUSSION

Taphonomic and early diagenetic processes during pre-depositional stage

Numerous biogenic particles occurring in the Cenomanian turbidite spicule-bearing sediments came from the northern shelves of the Carpathian basins. The position of these shelf areas is interpreted on the basis of palaeocurrent indicators (e.g., Książkiewicz, 1962). The composition of bioclasts, characterized by a large number of the fragmented (broken during transportation), calcified sponge spicules (Fig. 8) and calcareous benthic foraminifers, shows that they originated in the neritic zone of the shelves and on the upper slope of the Silesian Basin (summary in Bąk M. *et al.*, in press). The original opaline silica of the spicules was replaced by blocky calcite during the initial decay and/or early burial of the siliceous sponges, which had grown in the carbonate mud (Fig. 9). The various dimensions of calcite crystals, observable inside the moulds after the original spicules, display successive stages of crystallisation (Fig. 4B, C). Such calcitization of siliceous sponges concurrently with silica dissolution is a known phenomenon, documented mainly from modern and ancient shallow-water environments, including spiculitic carbonate mud-mounds and reefs (Froget, 1976; Land, 1976; Wiedenmayer, 1980; Reitner and Keupp, 1991; Reitner, 1993; Hammes, 1995; Reitner *et al.*, 1995; Warnke, 1995; Pisera, 1997; Neuweiler *et al.*, 1999; Kauffman *et al.*, 2000). The dissolution of the opaline silica of spicules and their replacement by calcium carbonate may have occurred both within the living sponge, and during its decay in the weakly cemented material, a few centimetres thick, associated with bacterial mats (Hartman, 1979; Pratt *et al.*, 1986; Bavestrello *et al.*, 1996). According to Fritz (1958), after the death of a sponge, the organic material putrefies. This process normally favours the precipitation of carbonate (calcite spar) within and around the sponge spicules. However, at the beginning, an initial transformation from opaline to microquartz silica takes place within the spicules (e.g., Hartman *et al.*, 1980; Olóriz *et al.*, 2003).

The post-mortem microborings of carbonate bioclasts (foraminiferal tests and echinoid plates), visible as a micritic halo in thin sections of the rocks, have been made by

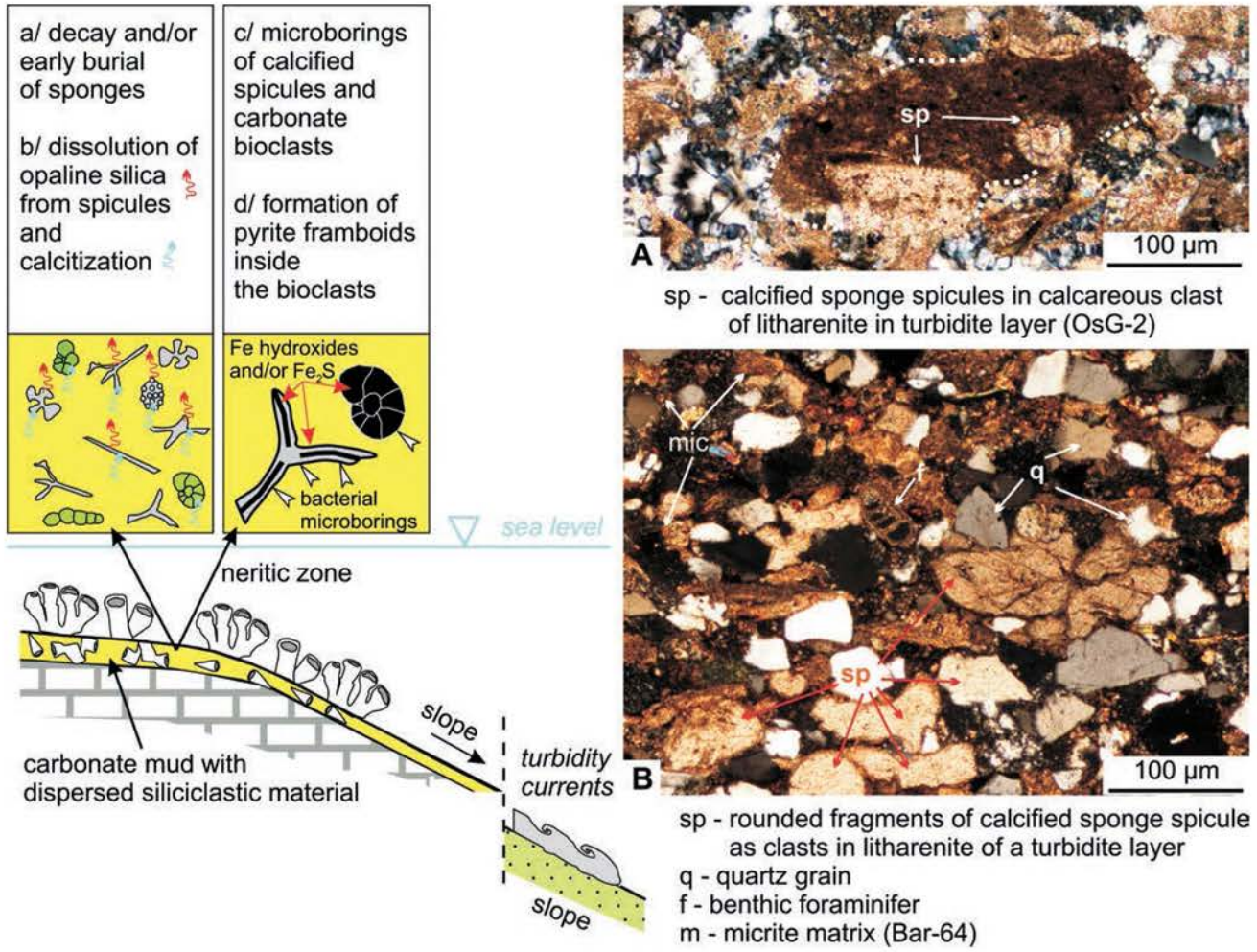

Fig. 9. An example of sequences of sedimentary and diagenetic events, interpreted on the basis of microfacies.

bacteria during taphonomic-early diagenetic processes, most probably in soft, poorly cemented carbonate mud (Bąk M. *et al.*, in press). Such corrosion of calcareous grains, caused by bacteria, is known from various modern and ancient environments (e.g., Lüttge and Conrad, 2004; Davis *et al.*, 2007). The same effect of bacterial corrosion is visible on the calcified spicules of sponges (Fig. 4I, J, O–R).

Another early diagenetic process, related to the shelf-derived bioclasts of the turbidites was the formation of spherical pyrite framboids, attached to the inner surfaces of planktonic and benthic foraminiferal tests. In some examples, growth of them took place also on the surfaces of the calcite rhombohedra inside the tests. The occurrence of such framboids is related to bacterial colonization, which may provide local nucleation sites for sulphides (e.g., Kaplan *et al.*, 1963; Ferris *et al.*, 1987; Kohn *et al.*, 1998). However, the pyritization inside the empty spaces in foraminiferal tests also could occur after their redeposition on the deep-sea basin floor. This cannot be unequivocally identified, because the subsequent processes related to dissolution of silica and calcitization also took place in the deep-sea environment.

These calcified spicules are found mostly in the T_b and T_c parts of the turbidite layers as fragmented particles, which are associated with siliciclastic (mainly quartz) grains. All of them have similar dimensions and occur in the micrite/clay matrix (Fig. 9B). In some turbidite layers, calcified sponge spicules have been redeposited in carbonate clasts (Fig. 9A). This shows on the one hand various stages of cementation of the carbonate mud on the shelf, and on the other, the occurrence of littoral currents on the shelf, which eroded the sea floor and transported the material toward the shelf break. It should be emphasized that among the redeposited sponge spicules, transported by littoral currents and turbidity currents, a large quantity of them were originally siliceous, but not those previously calcified in the shelf and upper-slope environments.

Diagenetic processes at deep basin floor

The mechanism of processes, related to the transportation of biogenic and siliciclastic particles from the shelf to the deep-basin floor, and the taphonomic processes on the basin floor are not discussed in this paper. However, it should be emphasised that the deposition of this material from turbidity currents took place most probably below the calcium compensation depth, as documented by the composition of benthic foraminiferal assemblages in the hemipelagic layers, intercalated with the spicule-bearing turbidites. They are devoid of calcareous benthos and are dominated

by deep-water agglutinated forms. Calcareous foraminiferal plankton was found only in the turbidites (Bąk M. *et al.*, 2005, 2011).

The next phase of diagenetic processes, which is discussed here, took place in the consolidated turbidite material, characterized by the occurrence of siliceous and calcareous bioclasts, siliciclastic grains, carbonate grains and micrite/clay matrix, related to the different compositions of the turbidites, giving rise to the various Bouma cycles. The earliest diagenetic process in such an environment was the dissolution of silica from the siliceous bioclasts in highly alkaline conditions, followed by early calcitization with the formation of rhombic calcite-like crystals, mostly inside and around the spicules (Fig. 5), the radiolarian and foraminiferal tests (Figs 4K, 7G, H) and also in the micritic matrix. These crystals were formed in conditions of high water content in the sediment, as was suggested previously by Mišik (1966, 1993), among others. The carbonate cementation was also related to the creation of spar crystals as an effect of micrite recrystallization. Such calcitization was described by many authors with regard to various environments (e.g., Dietrich *et al.*, 1963; Bustillo and Riuz-Ortiz, 1987; Gimenez-Montsant *et al.*, 1999). Most of the spicules preserved in the bioarenites, spiculitic sublitharenites and spiculites were calcified during this early diagenetic process. It occurs as selective calcitization during the early diagenetic interaction between the silica-rich fluids and the host sediment before later silicification.

Phases of silica cementations

Several phases of silica cementation occurred in these sediments after mechanical compaction and early calcitization (Figs 7G–K, 8C–F). The silicification was related to the creation of quartz overgrowths and precipitates as fibrous chalcedony (Fig. 7I, J) or microcrystalline quartz (Fig. K), derived from amorphous soluble kinds of silica (Fig. 8D–F). During this process, various forms of silica precipitates partially replaced calcite rhombohedra and micritic matrix, thus reducing the mouldic porosity after biogenic particles. Botryoidal chalcedony was formed in the initial stages (Fig. 8D), followed by microquartz (Fig. 8E) that enveloped the earlier material. The initial silicification could take place in an environment that was slightly acidic, where calcite could dissolve at the same time as silica was being precipitated, as was also discussed by Madsen and Stemmerik (2010) in a study of the diagenesis of flint and porcellanite in the Maastrichtian chalk. According to these authors, the dissolution of carbonate and liberation of magnesium hydroxyl complexes promoted the flocculation of silica that happened near to or at the surface of the dissolving carbonate, resulting in the silicification of microfossils, preserving their external shapes. In this replacement, rhombic dolomite crystals could be formed. The number of silicification phases, visible as different forms of silica precipitates inside the spicules (Figs 4M, N, 7C, D, 9), vary in particular turbidite layers; they are related to changes in many elements of the pore-water profile (see discussion in Mizutani, 1970; Knauth and Epstein, 1976; Knauth, 1994; Madsen and Stemmerik, 2010), which are not discussed here. The periodic sedimentation of turbidites containing different proportions of siliceous to carbonate particles might have changed, in a variety of ways, the conditions in the bottom and interstitial water, causing the re-establishment of a pore-water profile after deposition of the next turbidite layer.

Source of silica

The recent global estimates of silica budgets constructed for the world ocean show various sources of silica including fluxes related to biogenic silica production and recycling, biogenic silica burial in coastal regions, output fluxes related to reverse weathering in estuaries and to sponges, mineral weathering, dissolution of amorphous silica on ocean margins, and hydrothermal fluxes (e.g., Nelson *et al.*, 1995, Tréguer *et al.*, 1995; Tréguer and De La Rocha, 2013). Taking into account the character of the deposition of the sediments studied, which took place from diluted silty/sandy turbidity currents, and the composition of the shelf-derived particles in these turbidites (enriched in sponge spicules and radiolarians), transported to the deep-water basin floor below the calcium compensation depth, the authors suggest three main sources of silica in the bottom water. All of them resulted in the later silicification of these sediments. Two silica sources are related to the main biogenic components of the turbidites, i.e., to spicules of siliceous sponges and radiolarian skeletons. The third source may be connected with silica-rich hydrothermal vents.

A possible additional source might be diatom frustules. The occurrence of frustules has been documented in the claystone layers of these sediments (Bąk M., 2011). Today, diatoms are responsible for as much as 30–40% of the primary production at the modern ocean surface (Buesseler, 1998), and could have been a subordinate source of silica in the Upper Cenomanian part of the succession studied (Barnasiówka Radiolarian Shale Formation).

The radiolarian skeletons, initially composed of amorphous opal-A, could have great significance as a silica source in the Upper Cenomanian sediments. The redeposited radiolarian assemblages are numerous there in the turbidites. However, they are scarce in the hemipelagites, where there is a predominance of thick-walled skeletons, resistant to dissolution, or as skeletons replaced by pyrite or ferrous oxyhydroxides. The radiolarians which occur in the bottom sediments had to be transported through the water column in fecal pellets (Gersonde and Wefer, 1987; Bąk M., 2011). The pyrizited radiolarians found in the hemipelagites may indicate that the pellets were formed in waters which could have been periodically undersaturated with respect to silica. The rarity of siliceous radiolarian debris in the hemipelagites and their characteristic state of preservation in this sediment might be evidence of the early decay of such pellets during their descent in the water column and the progressive dissolution of the opaline radiolarian skeletons.

The preservation and/or dissolution of opaline radiolarian skeletons and sponge spicules might have been controlled by a few factors and processes (summary in DeMaster, 2003), including the variation in aluminium content (related to an occurrence of a thin dissolution-resistant, Al-rich opal layer in the siliceous skeletons; Van Cappelen and Qui, 1997a); changes in the specific surface areas of particles exposed to corrosive action during diagenesis; changes in pro-

tective organic coatings on fresh pellets including radiolarian skeletons in the water column; changes in bacterial type and their activity; differences in temperature and the degree of undersaturation; the effects of pH variations; and the sediment accumulation rate.

The latter factor could have been important in the silica diagenesis of the sediments studied, because it controlled the time of exposure of siliceous spicules and radiolarian skeletons to low saturation levels near the sediment-water interface. The biogenic silica preservation efficiencies, calculated for modern oceans in relation to various biogenic sources (e.g., DeMaster *et al.*, 1996) reveal large differences. Sponge spicules redissolve into silicic acid at far slower rates than those known for diatom frustules (Maldonado *et al.*, 2005). Similar data came from the laboratory analysis of the dissolution of radiolarian skeletons (Morley *et al.*, 2013). In both cases, there is non-linearity of silica dissolution with increasing depth, with the highest dissolution occurring at the water-sediment interface (Van Cappellen and Qui, 1997b; Gallinari *et al.*, 2002). Consequently, a low sedimentation rate with a low frequency of turbidite currents supplying siliceous bioclasts to the basin floor may favour the dissolution of siliceous bioclasts. This suggestion was also presented for the interpretation of initial silica precipitation in the North European epicontinental seas, where the occurrence of flint layers was correlated with omission surfaces and hardgrounds (e.g., Zijlstra, 1987). Following these observations and using data from similar chalk succession, Madsen and Stemmerik (2010) suggested that the initial precipitation of silica occurred near the seafloor during periods of slow or declining sedimentation. A similar conclusion is presented for the initial calcitization of bioclasts and precipitation of silica in relation to the sedimentation rate in the Mikuszowice Cherts studied. On the basis of biostratigraphical data from this succession (Bąk M. *et al.*, 2005; Bąk M., 2011), correlated with the chronostratigraphy, an average annual sedimentation rate for consolidated sediments of the Mikuszowice Cherts is estimated as 0.025 mm/yr and about 0.1 mm/yr for soft sediment. These are very low sedimentation rates, compared to the present-day environments of turbidite deposition (e.g., Piper and Deptuck, 1997).

As mentioned earlier, another source of silica on the seafloor of the Silesian Basin during the Middle–Late Cenomanian could be related to hydrothermal vents. The source for silicon in modern high-temperature (mid-ocean ridges) and low-temperature (ridge flanks) vents is suggested to have been a combination of seawater reaction with basalt and diffusive exchange with the overlying basal pore waters, which were in pseudo-equilibrium with amorphous silica (Wheat and McManus, 2005). In the modern oceans, the high-temperature hydrothermal systems, which leach silicon from the oceanic crust, resulting in high-silicic acid hydrothermal fluids, have a higher significance in silicon fluxes (Tréguer and De La Rocha, 2013). In this paper, the authors tentatively suggest that hydrothermal vents could be of some relevance in fluxes of dissolved silica to the seafloor during the Middle–Late Cenomanian, on the basis of chemical data from the overlying uppermost Cenomanian–lowermost Turonian sediments (the top of the Barnasiówka Radiolarian Shale Formation), which contain two horizons of Fe-Mn layers (Bąk K., 2007b). The chemical composition of these Fe-Mn sediments, characterized by low amounts of Co, Cu and Zn, a low Co/Zn ratio, a low Rare Earth Elements content with their characteristic distribution pattern, and proportions of Mn, Fe and (Ni+Cu+Co) that are typical for hydrothermal fields, may indicate a contribution of silicon from a hydrothermal source (Bąk K., 2006, 2007a–c).

FINAL REMARKS

The Cenomanian spicule-bearing turbidites in the flysch succession of the Silesian Nappe, in the Outer Carpathians, are highly silicified sediments, which contain numerous chert layers in the Middle–Upper Cenomanian part. They underwent several stages of diagenetic processes including the creation of various generations of cement and the dissolutions of various types of particle, which took place both before and after their deposition, and after their burial.

The first diagenetic changes, precluded by taphonomic processes, took place during the pre-depositional stage. These involved initial decay and/or early burial of sponge spicules and other microfossils within the spiculitic carbonate mud in the neritic zone of the northern shelves of the Outer Carpathian basins. In this environment, the calcitization of numerous siliceous sponge spicules and radiolarians took place. Opaline silica was replaced by blocky calcite and the skeletons of radiolarians and the tests of planktonic and benthic calcareous foraminifers were partly or entirely filled with calcite cements. Additionally, bacteria have corroded the calcified bioclasts. The pyrite framboids could have been formed on the inner surfaces of foraminiferal tests and voids after sponge spicules in small empty cavities with depleted oxygen content. However, this pyritization also could have been possible in a deep-sea environment.

After the transport of biogenic and siliciclastic particles from the shelves to the deep-basin floor below the CCD, and after taphonomic processes on this basin floor, later diagenetic processes of the bottom sediments were related to differences in the composition of successive turbidite flows.

Before the cementation of particles, mechanical compaction of the host sediment affected the spicule-bearing turbidites. After that, several alternating phases of carbonate and silica cementations, recrystallization and dissolution occurred in these sediments. During these phases, there was the formation of rhombic calcite-like crystals, especially inside of the calcareous or siliceous microplankton skeletons (tests), and the creation of spar crystals as an effect of micrite recrystallization. During silicification, various forms of silica precipitate replaced partially or entirely the calcite rhombohedra and micritic matrix and caused a reduction in the porosity after biogenic particles. These stages of silica *vs.* calcite dissolution, mobilization and crystalization were related to periodic sedimentation of successive turbidite, containing different proportion of siliceous to carbonates particles. It might have changed conditions in the bottom and interstitial water, causing the re-establishment of the pore-water profile after deposition of a next turbidite layer. The initial calcitization and precipitation of silica occurred

most probably near the seafloor, favoured by the low sedimentation rate, estimated as 0.1 cm/yr during Middle–Late Cenomanian.

Biogenic sources of silica may have caused the silicification of the sediments studied, including dissolution of primary siliceous sponge spicules, radiolarian skeletons and diatom frustules. However, a source from silica-rich hydrothermal vents was also possible, taking into account the published data on the uppermost Cenomanian–lowermost Turonian Fe-Mn sediments, which overlie the succession studied (Bąk K., 2006, 2007a–c). These vents were the sources of manganese and ferrous iron, precipitated on the basin floor and in the bottom sediments during that time.

Acknowledgements

We are grateful to Jozef Michalík, (Slovak Academy of Science, Geological Institute, Bratislava, Slovakia) and an anonymous reviewer for their helpful comments on the manuscript. Special thanks are to Przemysław Gedl, Frank Simpson and Alfred Uchman for their editorial work. The work was supported by funds from the AGH University of Science and Technology to M. Bąk (DS-AGH WGGiOŚ-KGOiG No 11.11.140.173), and Pedagogical University of Cracow to K. Bąk (DS-UP-WGB-3).

REFERENCES

Alexandrowicz, S. W., 1973. Gaize-type sediments in the Carpathian flysch. *Neues Jahrbuch für Geologie und Paläontologie, Monatshefte*, 1973(1): 1–17.

Baltuck, M., 1986. Authigenic silica in Tertiary and Upper Cretaceous sediments of the East Mariana Basin, Deep Sea Drilling Project Site 585. In: Moberly, R., Schlanger, S. O. *et al.* (eds), *Initial Reports of the Deep Sea Drilling Project*, 89: 389–398.

Bavestrello, G., Cattaneo-Vietti, R., Cerrano, C. & Sarŕ, M., 1996. Spicule dissolution in living *Tethya omanensis* (Porifera: Demospongiae) from a tropical cave. *Bulletin of Marine Science*, 58: 598–601.

Bąk, K., 2006. Sedimentological, geochemical and microfaunal responses to environmental changes around the Cenomanian–Turonian boundary in the Outer Carpathian Basin; a record from the Subsilesian Nappe, Poland. *Palaeogeography, Palaeoclimatology, Palaeoecology*, 237: 335–358.

Bąk, K., 2007a. Deep-water facies succession around the Cenomanian–Turonian boundary in the Outer Carpathian Basin: Sedimentary, biotic and chemical records in the Silesian Nappe, Poland. *Palaeogeography, Palaeoclimatology, Palaeoecology*, 248: 255–290.

Bąk, K., 2007b. Organic-rich and manganese sedimentation during the Cenomanian-Turonian boundary event in the Outer Carpathian Basin, a new record from the Skole Nappe, Poland. *Palaeogeography, Palaeoclimatology, Palaeoecology*, 256: 21–46.

Bąk, K., 2007c. Environmental changes during the Cenomanian–Turonian boundary event in the Outer Carpathian basins: a synthesis of data from various tectonic-facies units. *Annales Societatis Geologorum Poloniae*, 77: 171–191.

Bąk, K., Bąk, M. & Paul, Z., 2001. Barnasiówka Radiolarian Shale Formation – a new lithostratigraphic unit in the Upper Cenomanian–lowermost Turonian of the Polish Outer Carpathians. *Annales Societatis Geologorum Poloniae*, 71: 75–103.

Bąk, M., 2011. Tethyan radiolarians at the Cenomanian–Turonian Anoxic Event from the Apennines (Umbria-Marche) and the Outer Carpathians: Palaeoecological and Palaeoenvironmental implications. In: Tyszka, J. (ed.), *Methods and Applications in Micropalaeontology. Part II. Studia Geologica Polonica*, 134: 7–279.

Bąk, M., Bąk, K. & Ciurej, A., 2005. Mid-Cretaceous spicule-rich flysch deposits in the Silesian Nappe of the Polish Outer Carpathians; radiolarian and foraminiferal biostratigraphy. *Geological Quarterly*, 49: 275–290.

Bąk, M., Bąk, K. & Ciurej, A., 2011. Palaeoenvironmental signal from the microfossils record in the Mikuszowice Cherts of the Silesian Nappe, Polish Outer Carpathians. In: Bąk, M. Kaminski, M. A. & Waśkowska, A. (eds), *Integrating Microfossil Records from the Oceans and Epicontinental Seas. Grzybowski Foundation Special Publication*, 17: 15–25.

Bąk, M., Bąk, K., Górny Z. & Stożek B., in press. Evidence of bacteriogenic iron and manganese oxyhydroxides in Albian–Cenomanian marine sediments of the Carpathian realm (Poland). *Annales Societatis Geologorum Poloniae*.

Bryndal, T., 2014. A method for identification of small Carpathian catchments more prone to flash flood generation. Based on the example of south-eastern part of the Polish Carpathians. *Carpathian Journal of Earth and Environmental Sciences*, 9: 109–122.

Buesseler, K. O., 1998. The decoupling of production and particulate export in the surface ocean. *Global Biogeochemical Cycles*, 12: 297–310.

Burtan, J. & Skoczylas-Ciszewska, K., 1956. *Szczegółowa Mapa Geologiczna Polski, 1:50000, arkusz Bochnia*. Państwowy Instytut Geologiczny, Warszawa. [In Polish.]

Burtanówna, J., 1933. Der geologische Bau der Umgegend von Myślenice westlich vom Raba-Fluss. *Annales de la Société géologique de Pologne*, 9: 279–293.

Bustillo, M. A. & Riuz-Ortiz, P. A., 1987. Chert occurrences in carbonate turbidites: examples from the Upper Jurassic of the Betic Mountains (southern Spain). *Sedimentology*, 34: 611–662.

Cady, S. L., Wenk, H. R. & Downing, K. H., 1996. HRTEM of microcrystalline opal in chert and porcelanite from the Monterey Formation, California. *American Mineralogists*, 81: 1380–1395.

Calvert, S. E., 1971. Composition and origin of North Atlantic deep sea cherts. *Contribution to Mineralogy and Petrology*, 33: 273–288.

Calvert, S. E., 1974. Deposition and diagenesis of silica in marine sediments. *International Associations of Sedimentologists, Special Publication*, 1: 273–299.

Clayton, C. J., 1986. The chemical environment of flint formation in Upper Cretaceous chalks. In: Sieveking G. de C. & Hart, M. B. (eds), *The Scientific Study of Flint and Chert*. Cambridge University Press, Cambridge, pp. 43–54.

Davis, K. J., Nealson, K. H. & Luttge, A. 2007. Calcite and dolomite dissolution rates in the context of microbe–mineral surface interactions. *Geobiology*, 5: 191–205.

DeMaster , D. J., 2003. The diagenesis of biogenic silica: chemical transformations occurring in the water column, seabed, and crust. In: Holland, H. & Turekian, K. (eds), *Treatise on Geochemistry*, vol. 7. Elsevier Ltd., Amsterdam, pp. 87–98.

DeMaster, D. J., Ragueneau, O. & Nittrouer, C. A., 1996. Preservation efficiencies and accumulation rates for biogenic silica and organic C, N, and P in high-latitude sediments: the Ross Sea. *Journal of Geophysical Research*, 101: 18501–18518.

Dietrich, R., Hobbs, C. & Lowry, W., 1963. Dolomitization interrupted by silicification. *Journal of Sedimentary Petrology*, 33: 646–663.

Elorza, J. J. & Bustillo, M. A., 1989. Early and late diagenetic

chert in carbonate turbidites of the Senonian flysch, northeast Bilbao, Spain. In: Hein, J. R. & Obradović, J. (eds), *Siliceous Deposits of the Tethys and Pacific Regions*. Springer, New York, pp. 93–105.

Ferris, F. G., Fyfe, W. S. & Beveridge, T. J., 1987. Bacteria as nucleation sites for authigenic minerals in a metal-contaminated lake sediment. *Chemical Geology*, 63: 225–232.

Flörke, O. W., Graetsch, H., Martin, B., Röller, K. & Wirth, R., 1991. Nomenclature of microcrystalline and non-crystalline silica minerals, based on structure and microstructure. *Neues Jahrbuch für Mineralogie-Abhandlungen*, 163: 19–42.

Fritz, G. K., 1958. Schwammstozen, Tuberolithe und Schuttbreccien im Weissen Jura der Schwabischen Alb. *Arbeiten aus dem Geologisch-Paläontologischen Institut Technische Hochschule Stuttgart, N.F.*, 13: 1–118.

Froget, C., 1976. Observation sur l'altération de la silice et des silicates au cours de la lithification carbonatée (région Siculo-Tunisienne). *Géologie Méditerranéenne*, 3: 219–226.

Gallinari, M., Ragueneau, O., Corrin, L., DeMaster, D. J. & Treguer, P., 2002. The importance of water column processes on the dissolution properties of biogenic silica in deep-sea sediments I. Solubility. *Geochimica et Cosmochimica Acta*, 66: 2701–2717.

Geroch, S., Jednorowska, A., Książkiewicz, M. & Liszkowa, J. 1967. Stratigraphy based upon microfauna in the Western Polish Carpathians. *Instytut Geologiczny, Biuletyn*, 211: 185–282.

Gersonde, R. & Wefer, G., 1987. Sedimentation of biogenic siliceous particles in Antarctic waters from the Atlantic sector. *Marine Micropaleontology*, 11: 311–332.

Gimenez-Montsant, J., Calvet, F. & Tucker, M. E., 1999. Silica diagenesis in Eocene shallow-water platform carbonates, southern Pyrenees. *Sedimentology*, 46: 969–984.

Hammes, U., 1995. Initiation and development of small-scale sponge mud-mounds, Late Jurassic, Southern Franconian Alb, Germany. In: Monty, C. L. V., Bosence, D. W. J., Bridges, P. H. & Pratt, B. R. (eds), *Carbonate Mud-Mounds: Their Origin and Evolution. International Associations of Sedimentologists Special Publications*, 23: 335–357.

Hartman, W. D., 1979. A new sclerosponge from the Bahamas and its relationship to Mesozoic stromatoporoids. In: Lévi, C. & Boury-Esnault, N. (eds), *Biologie des Spongiaires - Sponge Biology. Colloques Internationaux du Centre National de la Recherche Scientifique*, 291: 467–474.

Hartman, W .D., Wendt, J .W. & Wiedenmayer, F., 1980. *Living and Fossil Sponges: Notes for a Short Course*. University of Miami, Miami, 274 pp.

Heaney, P. J., 1993. A proposed mechanism for the growth of chalcedony. *Contributions to Mineralogy and Petrology*, 115, 66–74.

Hesse, R., 1989. Silica diagenesis: origin of inorganic and replacement cherts. *Earth-Science, Reviews*, 26: 253–284.

Hurd, D. C., 1973. Interactions of biogenic opal, sediment and seawater in the central equatorial Pacific. *Geochimica et Cosmochimica Acta*, 37: 2257–2282.

Hurd, D. C., Pankratz, H. S., Asper, V., Fugate, J. & Morrow, H., 1981. Changes in the physical and chemical properties of biogenic silica from the central equatorial Pacific: Part III. Specific pore volume, mean pore size, and skeletal ultrastructure of acid-cleaned samples. *American Journal of Science*, 281: 833–895.

Kaplan, I. R., Emery, K. O. & Rittenberg, S. C., 1963. The distribution and isotopic abundance of sulphur in recent marine sediments off southern California. *Geochimica et Cosmochimica Acta*, 27: 297–331.

Kauffman, E. G., Herm, D., Johnson, C. C., Harries, P. & Efling, R. H., 2000. The ecology of Cenomanian lithistid sponge frameworks, Regensburg area, Germany. *Lethaia*, 33: 214–235.

Keene, J. B., 1975. Cherts and porcellanites from the north Pacific, DSDP LEG 32. In: Larson, R. L. & Moberly, R. *et al.* (eds), *Initial Reports of the Deep Sea Drilling Project*, 32: 429–507.

Knauth, L. P., 1994. Petrogenesis of chert. *Reviews in Mineralogy*, 29: 233–258.

Knauth, P. L. & Epstein, S., 1976. Hydrogen and oxygen isotope ratios in nodular and bedded cherts. *Geochemica et Cosmochemica Acta*, 40: 1095–1108.

Kohn, M. J., Riciputi, L. R., Stakes, D. & Orange, D. L., 1998. Sulfur isotope variability in biogenic pyrite: Reflections of heterogeneous bacterial colonization? *American Mineralogist*, 83: 1454–1468.

Koszarski, L. & Nowak, W., 1960. Comments to age of the Lgota Beds. *Kwartalnik Geologiczny*, 4: 468–483. [In Polish, with English summary.]

Koszarski, L. & Ślączka, A., 1973. Outer (flysch) Carpathians. Lower Cretaceous. In: Pożaryski, W. (ed.), *Geology of Poland*. Instytut Geologiczny, Warszawa, pp. 492–495.

Książkiewicz, M., 1951. *Objaśnienia do arkusza Wadowice. Szczegółowa Mapa Geologiczna Polski, 1:50 000*. Państwowy Instytut Geologiczny, Warszawa, 283 pp. [In Polish.]

Książkiewicz, M., 1956. Geology of the Northern Carpathians. *Geologische Rundschau*, 45: 396–411.

Książkiewicz, M. (ed.), 1962. *Geological Atlas of Poland; Stratigraphic and Facial Problems*, vol. 13. *Cretaceous and Older Paleogene in the Polish Outer Carpathians*. Instytut Geologiczny, Wydawnictwa Geologiczne, Warszawa, 20 maps, 20 pp. explanatory notes.

Land, L. S., 1976. Early dissolution of sponge spicules from reef sediments, North Jamaica. *Journal of Sedimentary Petrology*, 46: 967–969.

Lüttge, A. & Conrad, P. G., 2004. Direct observation of microbial inhibition of calcite dissolution. *Applied and Environmental Microbiology*, 70: 1627–1632.

Madsen, H. B. & Stemmerik, L., 2010. Diagenesis of flint and porcellanite in the Maastrichtian chalk at Stevns Klint, Denmark. *Journal of Sedimentary Research*, 80: 578–588.

Maldonado, M., Carmona, M. C., Velásquez, Z., Puig, M. A., Cruzado, A., López, A. & Young, C. M., 2005. Siliceous sponges as a Silicon sink: An overlooked aspect of benthopelagic coupling in the marine Silicon cycle. *Limnology and Oceanography*, 50: 799–809.

Mišik, M., 1966. *Microfacies of the Mesozoic and Tertiary Limestones of the West Carpathians*. Vydavatel'stvo Slovenskej Akademie Vied, Bratislava, 269 pp.

Mišik, M., 1993. Carbonate rhombohedra in nodular cherts: Mesozoic of the West Carpathians. *Journal of Sedimentary Research*, 63: 275–281.

Mizutani, S., 1970. Silica minerals in the early stage of diagenesis. *Sedimentology*, 15: 419–436.

Morley, J. J., Shemesh, A. & Abelmann, A., 2013. Laboratory analysis of dissolution effects on Southern Ocean polycystine Radiolaria. *Marine Micropaleontology*, 110: 83–86.

Nelson, D. M., Tréguer, P., Brzezinski, M. A., Leynaert, A. & Quéguiner, B., 1995. Production and dissolution of biogenic silica in the ocean: revised global estimates, comparison with regional data and relationship with biogenic sedimentation. *Global Biogeochemical Cycles*, 9: 359–372.

Neuweiler, F., Gautret, P., Thiel, V., Lange, R., Michaelis, W. & Reitner, J., 1999. Petrology of Lower Cretaceous carbonate mud mounds (Albian, N Spain): insights into organomineralic

deposits of the geological record. *Sedimentology*, 46: 837–859.

Okoński, S., Górny Z., Bąk M. & Bąk, K., 2014. Lithistid spicules in the sediments of the Turonian Variegated Shale in the Silesian Nappe, Polish Outer Carpathians. *Geology, Geophysics & Environment*, 40: 33–48.

Olóriz, F., Reolid, M. & Rodríguez-Tovar, F. J., 2003. A Late Jurassic carbonate ramp colonized by sponges and benthic microbial communities (External Prebetic, southern Spain). *Palaios*, 18: 528–545.

Oszczypko, N., 2004. The structural position and tectono-sedimentary evolution of the Polish Outer Carpathians. *Przegląd Geologiczny*, 52: 780–791.

Piper, D. J. W. & Deptuck, M., 1997. Fine-grained turbidites of the Amazon Fan: facies characterization and interpretation. In: Flood, R. D. *et al.* (eds), *Proceedings of the Ocean Drilling Program, Scientific Results*, 155: 79–108.

Pisera, A., 1997. Upper Jurassic siliceous sponges from the Swabian Alb: taxonomy and paleoecology. *Palaeontologia Polonica*, 57: 1–216.

Pisera, A. & Lévi, C. 2002. 'Lithistid' Demospongiae. In: Hooper, J. N. A. & Van Soest, R. W. M. (eds), *Systema Porifera: A Guide to Classification of Sponges*. Kluwer Academic/Plenum Publisher, New York, pp. 299–301.

Pratt, B., R., Bourque, P. A. & Gignac, H., 1986. Sponge-constructed stromatactis mud mounds, Silurian of Gaspe, Quebec; discussion and reply. *Journal of Sedimentary Research*, 56: 459–463.

Reitner, J., 1993. Modern cryptic microbialite-metazoan facies from Lizard Island (Great Barrier Reef, Australia) – formation and concepts. *Facies*, 29: 3–40.

Reitner, J. & Keupp, H., 1991. The fossil record of the Haplosclerid excavating sponge *Aka* de Laubenfels. In: Reitner, J. & and Keupp, H. (eds), *Fossil and Recent Sponges*, Springer Verlag, Berlin, pp. 102–120.

Reitner, J., Neuweiler, F. & Gautret, P., 1995. Modern and fossil automicrites: implications for mud-mound genesis. *Facies*, 32: 4–17.

Riech, V. & von Rad, U., 1979. Silica diagenesis in the Atlantic Ocean: diagenetic potential and transformations. In: Talwani, M., Hay, W. & Ryan, W. B. F. (eds), *Deep Drilling in the Atlantic Ocean: Continental Margins and Paleoenvironment*. American Geophysical Union, *Maurice Ewing Series*, 3, pp. 315–340.

Sujkowski, Z., 1933. Sur certains spongiolithes de la Tatra et des Karpates. *Państwowy Instytut Geologiczny*, *Sprawozdania*, 7: 712–733. [In Polish, with French summary.]

Tréguer, P., Nelson, D. M., van Bennekom, A. J., DeMaster, D. J., Leynaert, A. & Quéguiner, B., 1995. The balance of silica in the world ocean: a re-estimate. *Science*, 268: 375–379.

Tréguer, P. J. & De La Rocha, C. L., 2013. The World Ocean silica cycle. *Annual Review of Marine Science*, 5: 477–501.

Unrug, R., 1959. On the sedimentation of the Lgota beds. *Rocznik Polskiego Towarzystwa Geologicznego*, 29: 197–225. [In Polish, with English summary.]

Unrug, R., 1977. Ancient deep-sea traction currents deposits in the Lgota beds (Albian) of the Carpathian Flysch. *Rocznik Polskiego Towarzystwa Geologicznego*, 47: 355–370.

Van Cappellen, P. & Qui, L., 1997a. Biogenic silica dissolution in sediments of the Southern Ocean. II. Solubility. *Deep-Sea Research II*, 44: 1109–1128.

Van Cappellen, P. & Qui, L., 1997b. Biogenic silica dissolution in sediments of the Southern Ocean. II. Kinetics. *Deep-Sea Research II*, 44: 1129–1140.

Von Rad, U. & Rösch, H., 1972. Mineralogy and origin of clay minerals, silica and authigenic silicates in Leg 14 sediments. *Reports of Deep Sea Drilling Project*, 14: 727–751.

Von Rad, U. & Rösch, H., 1974. Petrography and diagenesis of deep-sea cherts from the central Atlantic. In: Hsu, K. J. & Jenkyns H. C. (eds), *Pelagic Sediments: On Land and Under the Sea*. Blackwell Scientific Publications, Oxford, pp. 327–347.

Warnke, K., 1995. Calcification processes of siliceous sponges in Viséan limestones (counties Sligo and Leitrim, Northwestern Ireland. *Facies*, 33: 215–228.

Wheat, C. G. & McManus, J., 2005. The potential role of ridge-flank hydrothermal systems on oceanic germanium and silicon balances. *Geochimica at Cosmochimica Acta*, 69: 2021–2029.

Wiedenmayer, F., 1980. Siliceous Sponges-development through time. In: Hartman, W. D., Wendt, J. W. & Wiedenmayer, F. (eds), *Living and fossil sponges. Notes for a short course. Sedimenta*, 8: 55–85.

Williams, L. A. & Crerar, D. A., 1985. Silica diagenesis: II. General mechanisms. *Journal of Sedimentary Petrology*, 55: 312–321.

Williams, L. A., Parks, G. A. & Crerar, D. A., 1985. Silica dia-ge nesis: I. Solubility controls. *Journal of Sedimentary Petrology*, 55: 301–311.

Wise, S. W. & de Weaver, F. M., 1974. Chertification of oceanic sediments. In: Hsu, K. J. & Jenkyns H. C. (eds), *Pelagic Sediments: On Land and Under the Sea*. Blackwell Scientific Publications, Oxford, pp. 301–326.

Zijlstra, H. J. P., 1987. Early diagenetic silica precipitation, in relation to redox boundaries and bacterial metabolism in Late Cretaceous chalk of the Maastrichtian type locality: *Geologie en Mijnbouw*, 66: 343–355.